

**図 4-7** 図 4-6 の症例での術前脳血流 SPECT の Z score 画像解析

(左: 安静時, 右: acetazolamide 負荷時で, 上段は脳表血流分布, 中段は全脳 (GLB) にて正規化した Z score の分布, 下段は小脳 (CBL) にて正規化した Z score の分布であり, それぞれ右外側 (LAT), 左外側 (LAT), 上方 (SUP) からみた脳表画像を示す.)

術前の Z score の分布では, 左側中大脳動脈領域において安静時の前頭・側頭・頭頂葉に Z score の高い (脳血流としては低下) 領域が認められ, acetazolamide 負荷時には同領域の Z score が安静時よりもさらに高い値となっている. 本例では, 安静時に Z score の高い領域, acetazolamide 負荷時に同領域の Z score のさらなる上昇が認められ, 血行力学的脳虚血の特徴がみられる.

虚血の重症度 Stage II の領域がそれぞれ定位的に示される. 術後は, 同じ血管支配域内の安静時脳血流, acetazolamide 負荷時の血管反応性, 脳循環予備能などの各指標がいずれも改善し, 血行力学的脳虚血の重症度が不均一ながら軽症化することが捉えられる. 本解析法により, 脳血流 SPECT の定位定量解析が可能となり, 血行力学的脳虚血の重症度評価の判定精度が改善し, 画像診断の標準化が進むものと考えられる.

図 4-9, 4-10 は図 4-6 の症例の術前術後における脳血流 SPECT をそれぞれ SEE 解析した結果である.

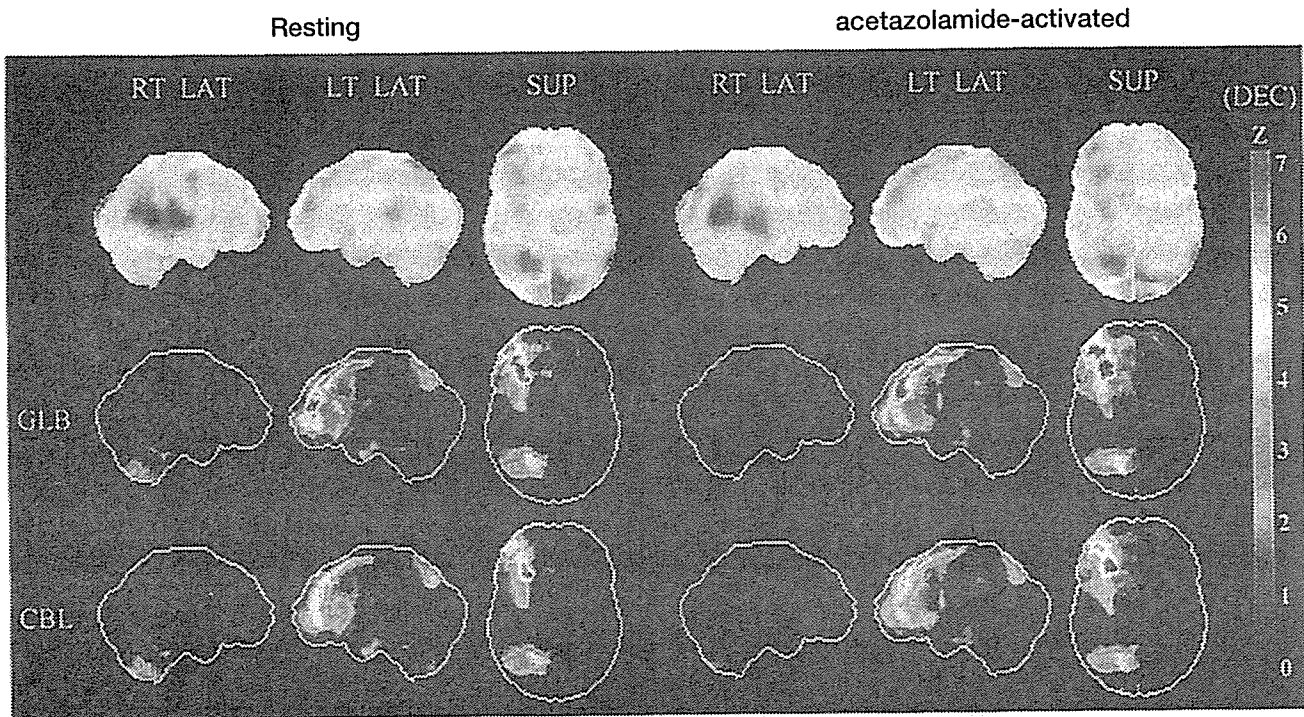


図 4-8 図 4-6 の症例での術後脳血流 SPECT の Z score 画像解析

(左: 安静時, 右: acetazolamide 負荷時で, 表示方法は図 4-7 と同様である.)

術後の Z score の分布では, 左側中大脳動脈領域において安静時の前頭・頭頂葉の一部に Z score の高い (脳血流としては低下) 領域が認められ, acetazolamide 負荷時には同じ領域に Z score の高い領域が認められるものの Z score の上昇はない。安静時に Z score の高い領域が認められても, acetazolamide 負荷時に同領域の Z score の上昇が認められないことは, 血行再建術後の血行力学的脳虚血の改善を示唆している。

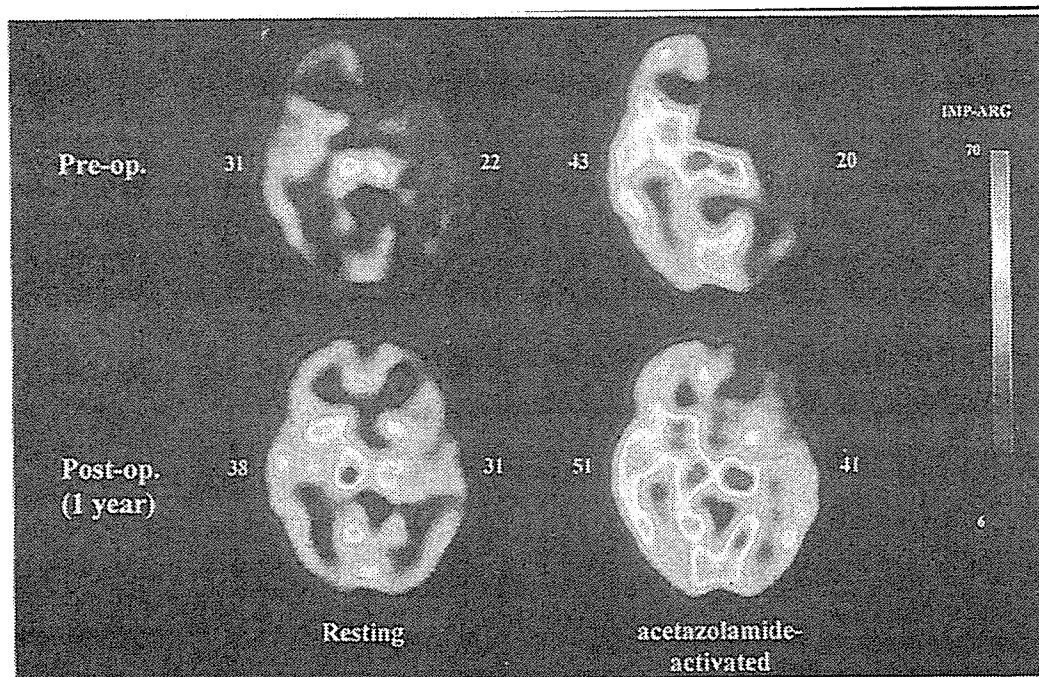


図 4-9 血行力学的脳虚血症例の脳血流 SPECT 定量画像解析

65 歳男性, 右片麻痺・言語障害にて発症した左内頸動脈閉塞症の術前安静時脳血流 SPECT の定量解析 (左上段), acetazolamide 負荷時脳血流 SPECT の定量解析 (右上段), 術後安静時脳血流 SPECT の定量解析 (左下段), acetazolamide 負荷時脳血流 SPECT の定量解析 (右下段) を示す。図 4-2 の評価基準により, 左側中大脳動脈領域が術前 Stage II, 術後 Stage I と判定される。



Rest: 991227\_65MIMPWSFM  
 Diamox: 991229\_65MIMPWSFM

magnification: 1.00  
 Rest CBF\*0.8: 34.0

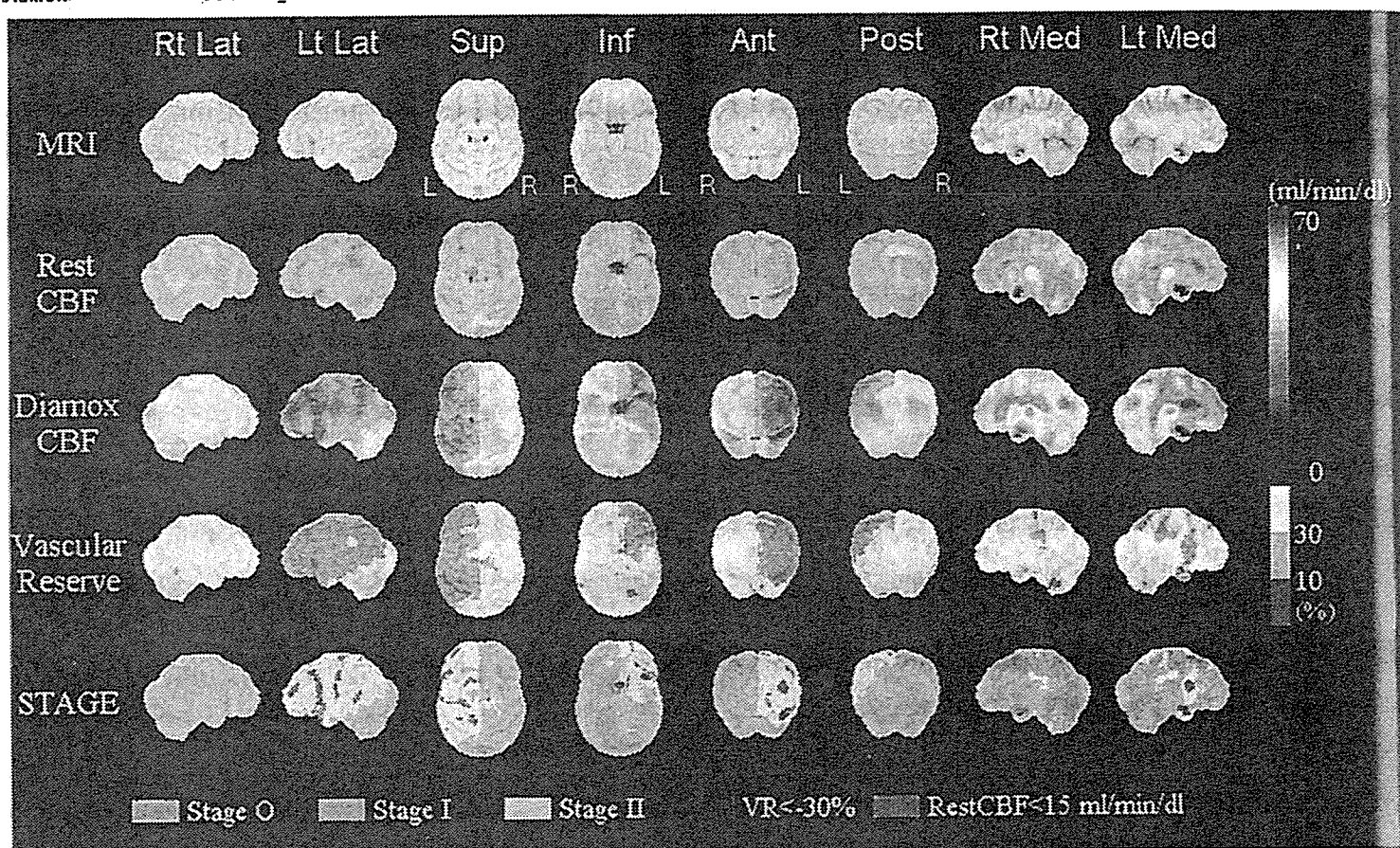


図 4-10 図 4-9 の症例での術前脳血流 SPECT の SEE 解析

(上段から、標準脳の MRI、安静時脳表血流量、acetazolamide 負荷脳表血流量、脳循環予備能、血行力学的脳虚血の Stage であり、それぞれ右外側 (Rt. Lat)、左外側 (Lt. Lat)、上方 (Sup)、下方 (Inf)、前方 (Ant)、後方 (Post)、右内側 (Rt. Med)、左内側 (Lt. Med) の 8 方向からみた脳表面画像を示す。)

中大脳動脈および前大脳動脈領域内に、安静時脳血流の低下領域、acetazolamide 負荷時の血管反応性の低下領域、脳循環予備能の低下領域、血行力学的脳虚血の重症度 Stage II の領域がそれぞれ定位的に示される。



## 慢性期脳血行再建術のガイドライン

Stroke prevention を目的とする STA-MCA バイパス術の現時点での適応基準は、JET Study<sup>7)</sup> に準じて以下の項目を満たす必要がある。①内頸動脈系の閉塞性血管病変 (アテローム血栓性) による TIA あるいは minor stroke を 3 カ月以内に認めた 73 歳以下の症例で、modified Rankin disability scale (mRS) が 1 あるいは 2 の症例であること。②放射線学的な基準としては、CT あるいは MRI 上 1 血管支配領域にわたる広範な脳梗塞巣を認めず、脳血管造影上内頸動脈あるいは中大脳動脈本幹の閉塞あるいは高度狭窄をもつ症例であること。③脳循環動態の基準としては、最終発作から 3 週間以上経過後に行った PET, SPECT ( $^{133}\text{Xe}$  あるいは

Rest: 000208\_65MIMPWSFM

magnification: 1.00

1.00

Diamox: 000210\_65MIMPWSFM

Rest CBF\*0.8:

34.0

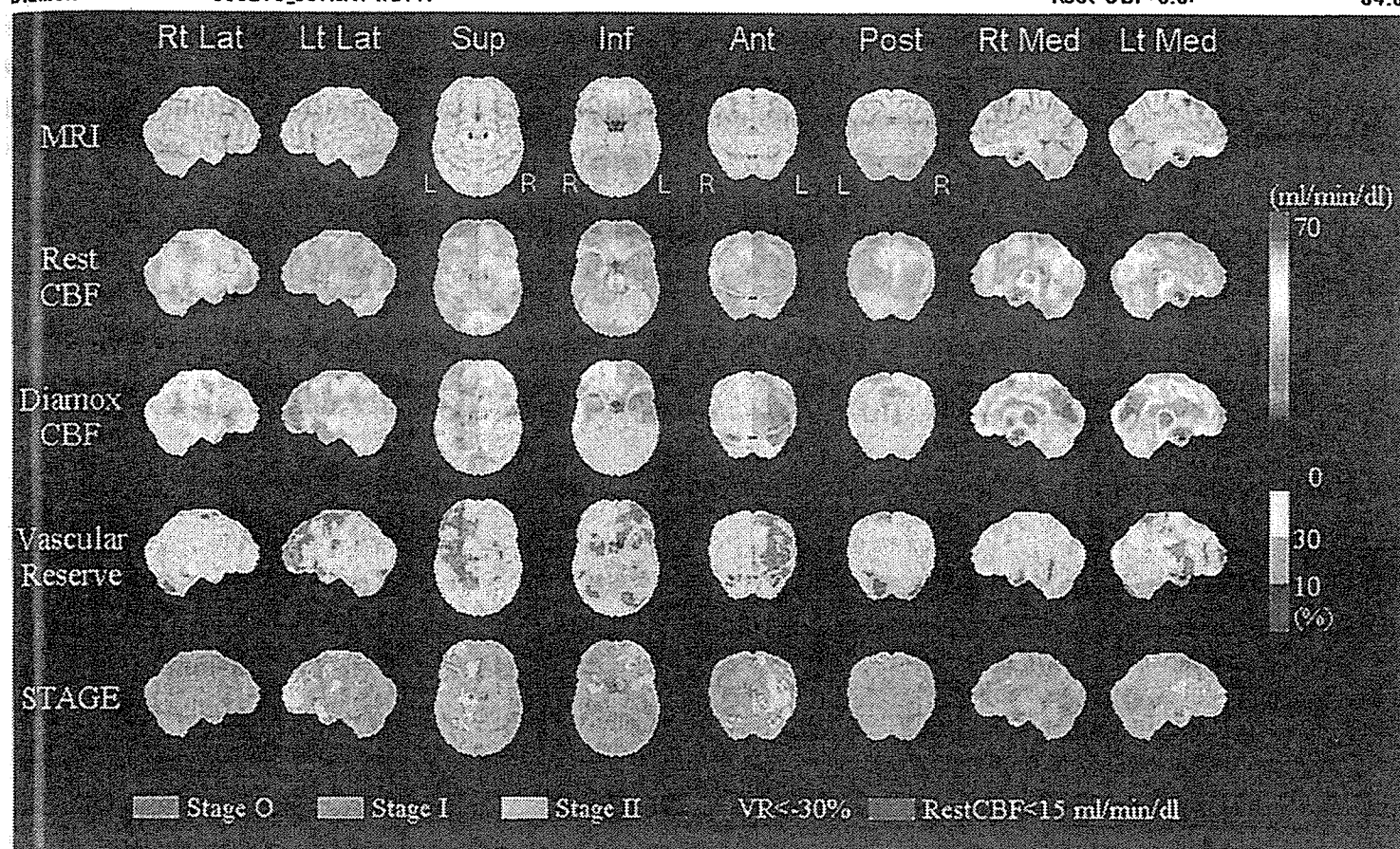


図 4-11 図 4-9 の症例での術後脳血流 SPECT の SEE 解析

(表示方法は図 4-10 と同様である.)

中大脳動脈および前大脳動脈領域内の安静時脳血流, acetazolamide 負荷時の血管反応性, 脳循環予備能などの各指標が術後いずれも改善し, 血行力学的脳虚血の重症度が不均一ながらも明らかに軽症化している. 本法では, 術前後における同一領域内の各 pixel における Stage の改善を定量的に判定できるとともに各 Stage の占める割合の変化を量的に算出し比較することも可能である.

$^{123}\text{I}$ IMP), あるいは cold Xe CT を用いた定量的な脳循環測定にて, 中大脳動脈領域の安静時脳血流が正常平均値の 80% 未満かつ脳循環予備能が 10% 以下の症例であること. 一方, 除外基準としては, ①神経症候が重症な症例 (mRS が 3 以上), ②非動脈硬化病変の症例, ③悪性腫瘍・腎不全・心不全・肝不全・呼吸不全の合併する症例, ④6 カ月以内の心筋梗塞を合併する症例, ⑤空腹時血糖値が 300 mg/dl 以上あるいはインスリン治療が必要となる症例, ⑥拡張期血圧が 110 mmHg 以上の症例, ⑦動脈原性脳塞栓症, ⑧心原性脳塞栓症, などがあげられる. また, このほか周術期の合併症を回避するためには, 術者の条件として本手術を十分習熟していること, 治療施設の条件として術後集中治療室において十分な術後管理ができること, などが重要である.

JET Study は, 血行力学的脳虚血 Stage II と診断される症例を対象とした場合において, Stroke prevention を目的とする STA-MCA バイパス術の有効性を示したものであり, より軽

症の血行力学的脳虚血に対する STA-MCA バイパス術の有効性は未だ確立していない。今後は、より軽症の血行力学的脳虚血を対象とした場合の STA-MCA バイパス術の有効性に関する検討が必要である。

## おわりに

Stroke prevention を目的とする STA-MCA バイパス術の有効性に関するエビデンスは、JET study によってようやく確認された。しかしながら、現在のところその適応は血行力学的脳虚血 Stage II と診断された subgroup に限られている。血行力学的脳虚血 Stage II に関する現在の基準は PET でなければ診断が困難と考えられた misery perfusion に相当する病態を診断するために想定された基準であり、より軽症の血行力学的脳虚血症例に対しても STA-MCA バイパス術が有効となる可能性はあるが、その有効性については新たな RCT によって検証されなければならない。手術適応の拡大解釈は、JET Study の意義を損なうものとして厳に慎まなければならない。

また、手術適応の判定においては血行力学的脳虚血の定量的重症度判定がきわめて重要であるが、各施設における血行力学的脳虚血の定量的測定法や判定法については、必ずしも標準化されていない。したがって、stroke prevention を目的とする STA-MCA バイパス術の現時点での有効性を普遍化するためには、脳血流量法の標準化による測定精度の向上・定位定量的画像解析法による判定精度の向上などが課題になるものと考えられる。

## 文献

- 1) The EC/IC Bypass Study Group. Failure of extracranial-intracranial arterial bypass to reduce the risk of ischemic stroke. Results of an international randomized trial. *N Engl J Med.* 1985 ; 313 : 1191-200.
- 2) Ausman JI, Diaz FG. Critique of the extracranial-intracranial bypass study. *Surg Neurol.* 1986 ; 26 : 218-21.
- 3) Awad IA, Spetzler RF. Extracranial-intracranial bypass surgery: a critical analysis in light of the international cooperative study. *Neurosurgery.* 1986 ; 19 : 655-64.
- 4) Day AL, Rhoton AL Jr, Little JR. The extracranial-intracranial bypass study. *Surg Neurol.* 1986 ; 26 : 222-6.
- 5) Sundt TM Jr. Was the international randomized trial of extracranial-intracranial arterial bypass representative of the population at risk? *N Engl J Med.* 1987 ; 316 : 814-6.
- 6) 中川 翼. 頭蓋外・内吻合術（バイパス手術）. In: 阿部 弘, 他, 編. 脳神経外科疾患の手術と適応 II. 東京: 朝倉書店; 1990. p.113-61.
- 7) JET Study Group. Japanese EC-IC Bypass trial (JET study) — Study design と中間解析結果—. 脳卒中の外科. 2002 ; 30 : 97-100.
- 8) Yonekawa Y, Yasargil MG. Extra-intracranial arterial anastomosis: Clinical and technical aspects. Result. In: Krayenbuhl H, editor. *Advances and technical standards of neurosurgery* 3, ed. Wien : Springer Verlag; 1976. p.47-78.
- 9) 菊池晴彦, 唐澤 淳. 脳血管閉塞症に対する浅側頭動脈—中大脳動脈側頭葉皮質枝吻合術. 脳神経外科. 1973 ; 1 : 15-9.
- 10) 米川泰弘. 頭蓋外内動脈吻合術の適応, 手技, 成績. *NEUROSURGEONS* 第 1 回日本脳神経外科

- 11) Khodadad G. Occipital artery-posterior inferior cerebellar artery anastomosis. Surg Neurol. 1976 ; 5 : 225-7.
- 12) Sundt TM Jr, Piepgras DG. Occipital to posterior inferior cerebellar artery bypass surgery. J Neurosurg. 1978 ; 48 : 916-28.
- 13) Ausman JI, Lee MC, Chater N, et al. Superficial temporal to superior cerebellar artery anastomosis for distal basilar artery stenosis. Surg Neurol. 1979 ; 12 : 277-82.
- 14) Ausman JI, Diaz FG, de los Reyes RA, et al. Boulos R. Anastomosis of occipital artery to anterior inferior cerebellar artery for vertebrobasilar junction stenosis. Surg Neurol. 1981 ; 16 : 99-102.
- 15) 菊池晴彦, 唐澤 淳, 永田 泉. 脳動脈の微小血管吻合術 後頭動脈・後下小脳動脈吻合術. 脳神経外科. 1983 ; 11 : 1023-5.
- 16) Ausman JI, Diaz FG, Vacca DF, et al. Superficial temporal and occipital artery bypass pedicles to superior, anterior inferior, and posterior inferior cerebellar arteries for vertebrobasilar insufficiency. J Neurosurg. 1990 ; 72 : 554-8.
- 18) 小川 彰, 吉本高志, 桜井芳明. 後頭蓋窩血行再建術—浅側頭動脈—上小脳動脈吻合術—. 脳外誌. 1992 ; 1 : 20-4.
- 19) 上山博康. 橈骨動脈を用いたバイパス手術. 脳神経外科. 1994 ; 22, 911-24.
- 20) National Institute of Neurological Disorders and stroke Ad Hoc Committee: Classification of cerebrovascular disease III. Stroke. 1990 ; 21 : 637-76.
- 21) Powers WJ, Grubb RL Jr, Raichle ME. Physiological responses to focal cerebral ischemia in humans. Ann Neurol. 1984 ; 16 : 546-52.
- 22) Baron JC, Boussier MG, Rey A, et al. Reversal of "misery perfusion syndrome" by extra-intracranial arterial bypass in hemodynamic cerebral ischemia: a case study with <sup>15</sup>O positron emission tomography. Stroke. 1981 ; 12 : 454-9.
- 23) 中川原譲二. SPECT と PET. In: 山口武典, 他, 編. 脳卒中学 The Frontiers of Strokeology. 東京: 医学書院; 1998. p.139-54.
- 24) Samson Y, Baron JC, Boussier MG, et al. Effects of extra-intracranial arterial bypass on cerebral blood flow and oxygen metabolism in humans. Stroke. 1985 ; 16 : 609-16.
- 25) Iida H, Itoh H, Nakazawa M, et al. Quantitative mapping of regional cerebral blood flow using iodine-123-IMP and SPECT. J Nucl Med. 1994 ; 35 : 2019-30.
- 26) 飯田秀博. IMP-ARG 法. 西村恒彦, 編, SPECT 機能画像—定量化の基礎と臨床—東京: メジカルビュー社; 1999. p.72-8
- 28) 中川原譲二. 脳虚血の臨床画像診断. 脳と神経. 1999 ; 51 : 502-13.
- 29) 中川原譲二, 新谷朋子, 氷見徹夫, 他. 脳血流 SPECT の最新の画像解析とその臨床的意義. 脳外誌. 2000 ; 9: 483-90.
- 30) Yonas H, Smith HA, Durham SR, et al. Increased stroke risk predicted by compromised cerebral blood flow reactivity. J Neurosurg. 1993 ; 77 : 483-9.
- 31) Yamauchi H, Fukuyama H, Nagahama Y, et al. Evidence of misery perfusion and risk for recurrent stroke in major cerebral arterial occlusive diseases from PET. J Neurol Neurosurg Psychiatry 1996 ; 61 : 18-25.
- 32) Grubb RL Jr, Derdeyn CP, Fritsch SM, et al. Importance of hemodynamic factors in the prognosis of symptomatic carotid occlusion. JAMA. 1998 ; 280 : 1055-60.
- 33) Derdeyn CP, Grubb RL Jr, Powers WJ. Cerebral hemodynamic impairment: methods of measurement and association with stroke risk. Neurology. 1999 ; 53 : 251-9.
- 34) Kuroda S, Houkin K, Kamiyama H, et al. Long-term prognosis of medically treated patients with internal carotid or middle cerebral artery occlusion: can acetazolamide test predict it? Stroke. 2001 ; 32 : 2110-6.

- 35) Macdonald RL. Advances in vascular surgery. Stroke. 2004 ; 35 : 375-80.
- 36) Iida H, Akutsu T, Endo K, et al. A multicenter validation of regional cerebral blood flow quantitation using [ $^{123}\text{I}$ ] iodoamphetamine and single photon emission computed tomography. J Cereb Blood Flow Metab. 1996 ; 16 : 781-93.
- 37) Renkin EM. Regulation of the microcirculation. Microvasc Res 1985 ; 30 : 251-63.
- 38) Kuhl DE, Barrio JR, Huang SC, et al. Quantifying local cerebral blood flow by N-isopropyl- $\rho$ - [ $^{123}\text{I}$ ] iodoamphetamine (IMP) tomography. J Nucl Med. 1982 ; 23 : 196-203.
- 39) Imaizumi M, Kitagawa K, Hashikawa K, et al. Detection of misery perfusion with split-dose  $^{123}\text{I}$ -Iodoamphetamine single-photon emission computed tomography in patients with carotid occlusive diseases. Stroke 2002 ; 33 : 2217-23.
- 40) Friston KJ, Holmes AP, Worsley KJ, et al. Statistical parametric maps in functional imaging: A general linear approach. Human Brain Mapping. 1995 ; 2 : 189-210.
- 41) Minoshima S, Frey KA, Koeppe RA, et al. A diagnostic approach in Alzheimer's disease using three-dimensional stereotactic surface projections of fluorine-18-FDG PET. J Nucl Med. 1995 ; 36 : 1238-48.
- 42) Mizumura S, Nakagawara J, Takahashi M, et al. Three-dimensional display in staging hemodynamic brain ischemia for JET study: Objective evaluation using SEE analysis and 3D-SSP display. Ann Nucl Med. 2004 ; 18 : 13-21.
- 43) Minoshima S, Giordani B, Berent S, et al. Metabolic reduction in the posterior cingulate cortex in very early Alzheimer's disease. Ann Neurol. 1997 ; 42 : 85-94.

〈中川原譲二〉



## Altered expression balance of matrix metalloproteinases and their inhibitors in human carotid plaque disruption: Results of quantitative tissue analysis using real-time RT-PCR method

Takeo Higashikata<sup>a</sup>, Masakazu Yamagishi<sup>a,\*</sup>, Toshio Higashi<sup>b</sup>, Izumi Nagata<sup>b</sup>, Koji Iihara<sup>b</sup>,  
Susumu Miyamoto<sup>b</sup>, Hatsue Ishibashi-Ueda<sup>c</sup>, Noritoshi Nagaya<sup>d</sup>,  
Takashi Iwase<sup>d</sup>, Hitonobu Tomoike<sup>a</sup>, Aiji Sakamoto<sup>e</sup>

<sup>a</sup> Division of Cardiovascular Medicine and Bioscience, National Cardiovascular Center and Research Institute,  
5-7-1 Fujishiro-dai, Suita, Osaka 565-8565, Japan

<sup>b</sup> Division of Neurosurgery, National Cardiovascular Center, Suita, Osaka, Japan

<sup>c</sup> Division of Pathology, National Cardiovascular Center, Suita, Osaka, Japan

<sup>d</sup> Division of Regenerative Medicine and Tissue Engineering, National Cardiovascular Center and Research Institute, Suita, Osaka, Japan

<sup>e</sup> Division of Biotechnology and Bioscience, National Cardiovascular Center and Research Institute, Suita, Osaka, Japan

Received 28 October 2004; received in revised form 17 May 2005; accepted 27 May 2005

Available online 21 July 2005

### Abstract

**Background:** The balance between degradation and synthesis of extracellular matrix determines its content in atherosclerotic tissue. To examine the role of expression balance of matrix metalloproteinases (MMPs) to their inhibitors, tissue inhibitors of metalloproteinases (TIMPs) and tissue factor pathway inhibitor-2 (TFPI-2) in the development and disruption of atherosclerotic plaque, these gene expressions in human carotid plaque were quantitatively determined by real-time reverse transcription (RT)-polymerase chain reaction (PCR) method.

**Methods:** Total RNA for cDNA synthesis was extracted from tissues in 24 patients with carotid endarterectomy. The amounts of cDNAs for MMP-1, -2, -3 and -9, TFPI-2 and TIMP-1, -2 and -3 were determined by real-time RT-PCR method, and normalized with glutaraldehyde 3-dehydrogenase.

**Results:** In plaques, the expression MMP-1 ( $1.53 \pm 0.25$ , mean  $\pm$  S.E.M.), MMP-3 ( $1.99 \pm 0.59$ ) and MMP-9 ( $2.00 \pm 0.51$ ) was augmented compared to those in the adjacent control regions ( $0.60 \pm 0.16$ ,  $0.46 \pm 0.18$  and  $0.58 \pm 0.21$ , respectively,  $p < 0.05$ ). The expression of TFPI-2 was lower in plaques ( $0.32 \pm 0.08$ ) than in controls ( $0.94 \pm 0.23$ ,  $p < 0.01$ ). Although the expression of TIMP-1 was higher in plaques ( $1.28 \pm 0.23$ ) than in controls ( $0.81 \pm 0.10$ ,  $p < 0.05$ ), the indices of MMP-1/TIMP-1, MMP-3/TIMP-3 and MMP-9/TIMP-1 were still significantly higher in plaques. Interestingly, MMP-9 and the resulting MMP-9/TIMP-1 balance in plaques with disruption were significantly higher ( $3.36 \pm 1.52$  and  $1.66 \pm 0.12$ ,  $n = 11$ ) than those in non-disrupted plaques ( $1.11 \pm 0.52$  and  $0.76 \pm 0.12$ ,  $n = 13$ ,  $p < 0.05$ ).

**Conclusion:** With the decreased expression of TFPI-2, upregulation of MMPs in atherosclerotic plaque was disproportional to that of TIMPs, suggesting that imbalanced degradation and synthesis of extracellular matrix persists in advanced lesions, particularly in plaques with disruption.

© 2005 Elsevier Ireland Ltd. All rights reserved.

**Keywords:** Atherosclerosis; Extracellular matrix; Matrix metalloproteinases; Tissue inhibitor of metalloproteinases; Tissue factor pathway inhibitor-2; Plaque disruption

### 1. Introduction

Disruption of atherosclerotic plaque during its development can expose the thrombogenic core to luminal blood flow, frequently resulting in ischemic cardiac events and stroke

\* Corresponding author. Tel.: +81 6 6833 5012; fax: +81 6 6833 9865.  
E-mail address: myamagi@hsp.ncvc.go.jp (M. Yamagishi).



[1,2]. During this process, structural changes in extracellular matrix (ECM) were shown to play a crucial role in plaque development and disruption [3]. The structural integrity of plaques seems to depend on a balance between synthesis and degradation of the ECM which is mainly regulated by proteinases such as matrix metalloproteinases (MMPs) including interstitial collagenase or MMP-1, gelatinase A or MMP-2, stromelysin 1 or MMP-3, gelatinase B or MMP-9 [4,5].

The activities of MMPs are controlled on multiple levels: transcription and translation of their inactive precursors (zymogens), post-translational activation of zymogens by proteolysis and interactions with tissue inhibitors of metalloproteinases (TIMPs) [6] and/or tissue factor pathway inhibitor-2 (TFPI-2) [7]. Indeed, TIMPs-1, -2, -3 and TFPI-2 are expressed in atherosclerotic lesions [7–9], and these inhibitors bind to and inactivate most of the MMPs [7,10]. Thus, the expression balance of MMP to TIMP and TFPI-2 is considered to regulate the net degeneration of ECM, thus contributing to maintaining plaque stability [7,11,12]. However, few systematic data exist regarding quantitative evaluation of the expression of MMPs and their inhibitors in human atherosclerotic plaques, probably because of technical difficulties in simultaneous determination of multiple gene expression in small tissue samples obtained in clinical settings. In the present study, we used real-time reverse transcription (RT)-polymerase chain reaction (PCR) and analyzed gene expression levels of MMPs, TIMPs and TFPI-2 in human carotid plaque and an adjacent control region. We also compared expression and function of MMPs between histologically disrupted and non-disrupted plaques.

## 2. Subjects and methods

### 2.1. Subjects

The protocol of this study was approved by the institutional committee for ethical review. Written informed consent was obtained from all 24 patients who underwent carotid endarterectomy for severe stenosis of the extracranial carotid artery (all male with mean age of  $68 \pm 2$

years). All patients presented clinical symptoms of cerebral ischemic attack related to carotid stenosis. Seven patients had a history of recent ischemic attack within 1 month prior to endarterectomy. The prevalence of risk factors for atherosclerosis was as follows: hypertension (systolic pressure  $>160$  mmHg) in 20, hyperlipidemia (total cholesterol  $>220$  mg/dl) in 22, smoking in 15 and diabetes mellitus (fasting blood glucose  $>110$  mg/dl) in 10 patients. High sensitive (hs) CRP level (normal range  $<3$  mg/l) just before surgery was  $2.45 \pm 0.43$  mg/l (Table 1).

### 2.2. Tissue sampling

Samples of the plaque region were obtained immediately after endarterectomy. Endarterectomy was extended in a caudal direction to include a sample of minimally affected common carotid artery proximal to the plaque but in continuity with the plaque to act as a paired control. Under these conditions, the stenotic segment and adjacent areas were dissected undisruptedly as a single specimen, preserving circumferential integrity as much as possible. Also special care was taken not to damage luminal surface and plaque interior. After removing a part of the tissue for histological examination, all samples were immediately frozen in liquid nitrogen and stored at  $-80^\circ\text{C}$  until extraction of mRNA.

Procedures for RNA preparation and cDNA synthesis were already described elsewhere in detail [13]. Briefly, the samples were homogenized in 1.0 ml ISOGEN<sup>TM</sup> reagent (Nippon Gene, Tokyo, Japan), thoroughly mixed with 0.2 ml chloroform and centrifuged at  $15,000 \times g$  for 15 min at  $4^\circ\text{C}$ . The aqueous supernatant was transferred into a micro test tube, mixed with 0.6 ml isopropanol and centrifuged at  $15,000 \times g$  for 15 min at  $4^\circ\text{C}$ . The precipitated total RNA was rinsed with 70% ethanol, air-dried and then resuspended in RNase-free water. Then, all the total RNA was treated with DNase Free<sup>TM</sup> reagent (Ambion, Austin, TX) for 60 min, and then reverse-transcribed with Superscript II<sup>TM</sup> (Invitrogen, Carlsbad, CA) at  $37^\circ\text{C}$  for 60 min using random primers (TaKaRa, Tokyo, Japan). The integrity of each cDNA mixture was checked by amplification of glutaraldehyde 3-phosphate dehydrogenase (GAPDH) with *ExTaq* (TaKaRa), using the primer set 5'-ACCACAGTCCATGCCATCAC-3'/5'-TCCACCACCCTGTTGCTGTA-3'.

Table 1  
Patient Characteristics

	All patients (n = 24)	With disruption (n = 11)	Without disruption (n = 13)	p-Value
Age	$68 \pm 2$	$66 \pm 3$	$69 \pm 2$	NS
Male sex	24	11	13	NS
Hypertension	20	8	12	NS
Diabetes	10	5	5	NS
HbA1c (%)	$6.5 \pm 0.4$	$7.0 \pm 0.8$	$6.2 \pm 0.4$	NS
Hyperlipidemia	22	9	13	NS
LDL (mg/dl)	$132 \pm 6$	$140 \pm 10$	$128 \pm 7$	NS
Smoking	15	5	10	NS
hs-CRP (mg/l)	$2.45 \pm 0.43$	$2.68 \pm 0.49$	$2.12 \pm 0.81$	NS

### 2.3. Primers and probes for real-time RT-PCR

Using Primer Express™ software (Applied Biosystems, Foster, CA), primers were designed for each of the genes for MMP-1, -2, -3 and -9, TFPI-2 and TIMP-1, -2 and -3, and the TaqMan probe inherent to each primer set was prepared, which was an oligonucleotide labeled with a reporter dye (FAM) at the 5'-end and a quencher dye (TAMRA) at the 3'-end. The sequences of the primers and TaqMan probes of MMPs-1, -2, -3, -9, TIMPs-1, -2 and -9 were reported elsewhere [13], and those for TFPI-2 were SENSE=CGATGCTTGCTGGAGGATAGA; ANTISENSE=ACAC-TGGTCGTCCACACTCACT; Taqman probe=5'-FAM-AAGTTCCTCCAAAGTTTGCCGGCTGC-TAMRA-3'; TFPI-2 SENSE=CGATGCTTGCTGGAGGATAGA; ANTI-SENSE=ACACTGGTCGTCCACACTCACT; Taqman probe=5'-FAM-AAGTTCCTCCAAAGTTTGCCGGCTGC-TAMRA-3'.

Real-time RT-PCR was performed using an ABI PRISM 7700 Sequence Detection System (Applied Biosystems). The reaction solution was assembled in a volume of 25  $\mu$ l, which comprised TaqMan Universal PCR Master Mix (Applied Biosystems), forward and reverse primers (final concentration 300 nM each), TaqMan probe (final concentration 200 nM) and cDNA mixture (about 2.5 ng). Throughout this study, the cDNA mixture from a particular sample was used to generate the working standard for quantitation of the cDNA of interest, which plots the relationship between the dilution of the standard cDNAs and the corresponding  $C_t$  value (the number of cycles necessary to obtain a threshold fluorescent signal) [13]. The initial quantity of the cDNA of interest in a certain cDNA mixture was calculated from the working standard and then normalized to that of GAPDH determined with TaqMan Assay Reagent Endogenous Control™ (Applied Biosystems). The normalized value for each target cDNA reflects the expression level of the corresponding gene in a test sample relative to the standard tissue. The accuracy of the present real-time RT-PCR for determining mRNA expression in human vascular tissue was already confirmed by comparing the results with those determined by conventional RT-PCR method [13].

### 2.4. Expression and function of MMP

To determine expression and function of MMP in its protein level, carotid tissue samples from 10 patients, in whom enough amounts of proteins could be extracted, were examined by Western blotting and gel zymography. The extracted protein was separated by SDS-PAGE and blotted onto a Hybond-ECL nitrocellulose membrane (Amersham) with the use of primary (40  $\mu$ g/ml) and secondary (1:2000, Amersham) antibodies. As for zymography, proteins with gelatinolytic activity were identified by use of substrate gels prepared by incorporation of gelatin (1 mg/ml; Wako) into a SDS-PAGE. After electrophoresis, gels were washed in 2.5% Triton X-100 for 30 min to remove SDS. The gel was equili-

brated for 30 min at room temperature with gentle agitation then incubated for overnight at 37 °C in 50 mM Tris/HCl, pH 7.5, containing 0.2 M NaCl, 5 mM CaCl<sub>2</sub> and 0.02% Brij 35. Gels were then fixed and stained with 0.25% Coomassie Brilliant Blue R-250 (Wako). The product of the optical net density of the band was compared with a positive control (HT-1080 human fibrosarcoma cells for Western blotting and human MMP-2 and human MMP-9, 1.5 ng, CC073; CHEMI-CON for zymography) to obtain a ratio comparable between gels.

### 2.5. Histology and immunohistochemistry

A part of the plaque was placed in tissue fixative (Histochoice, Hedwin, Baltimore). After overnight fixation, the samples were paraffin embedded and sectioned at 4- $\mu$ m intervals. Tissue sections were deparaffinized with xylene followed by immersion in graded alcohol. They were washed three times for 5 min each in phosphate-buffered saline (PBS) and blocked with bovine serum albumin for 60 min. Specimens were then incubated with primary antibodies against CD-68, MMPs, TIMPs and TFPI-2 (Fuji Chemical, Tokyo, Japan) overnight at 4 °C. After they were washed in PBS, specimens were incubated with biotinylated rabbit anti-mouse IgG for 60 min at room temperature. Specimens were then washed with PBS, stained with horseradish peroxidase-conjugated streptavidin, and finally incubated with substrate solution for 1–15 min. The tissue sections were also stained with hematoxylin–eosin and elastica van Gieson for evaluation of plaque composition and fibrous cap disruption, as described by Carr et al. [2]. Plaque was defined as atheromatous if the area of lipid core was  $\geq 30\%$  of the whole plaque area and as fibrous plaque if  $<30\%$  in terms of its vulnerability [14].

### 2.6. Data analysis

The mean and standard error of triplicate data are presented. Statistical analysis was performed by paired *t*-test using Stat View 5.0 software on a Macintosh computer and by Wilcoxon matched-pair signed-rank test if appropriate. A *p*-value  $<0.05$  was considered significant.

## 3. Results

### 3.1. Patient and plaque characteristics

Atheromatous plaque was observed in 15 samples and fibrous plaque in 9 samples. Disruption of the fibrous cap was observed in 11 samples with atheromatous plaque and was not observed in 13 samples, which consisted of 4 atheromatous and 9 fibrous plaques. Although levels of HbA1c and LDL-cholesterol in patients with plaque disruption tended to be higher than those in patients without disruption, there was no statistically significant difference in their clinical back-

Table 2  
MMP, TFPI-2 and TIMP levels

Mrna	Control	Plaque	p-Value
MMP-1	0.60 ± 0.16	1.53 ± 0.25	<0.01
MMP-2	0.80 ± 0.11	0.88 ± 0.14	NS
MMP-3	0.46 ± 0.18	1.99 ± 0.59	<0.05
MMP-9	0.58 ± 0.21	2.00 ± 0.51	<0.01
TFPI-2	0.94 ± 0.23	0.32 ± 0.08	<0.01
TIMP-1	0.81 ± 0.10	1.28 ± 0.23	<0.05
TIMP-2	1.12 ± 0.15	0.95 ± 0.17	NS
TIMP-3	0.47 ± 0.16	0.67 ± 0.17	NS

ground. Also there was no difference in hs-CRP level between two patient groups, although mean value in all patients was higher than normal value (Table 1).

### 3.2. Expression levels of MMPs, TIMPs and TFPI-2

From removed samples with a wet weight of  $11.69 \pm 2.64$  mg,  $0.49 \pm 0.22$   $\mu$ g total RNA was extracted for analysis. Amplification of GAPDH was equivalent among all the cDNAs synthesized. Each primer set for PCR exponentially amplified its target cDNA according to the cycle number. Normalized values for MMP, TIMP and TFPI-2 gene expression in plaque and adjacent control tissue (controls) are summarized in Table 2. In the plaques, the gene expression levels of MMP-1 ( $1.53 \pm 0.25$ ), MMP-3 ( $1.99 \pm 0.59$ ) and MMP-9 ( $2.00 \pm 0.51$ ) were significantly higher than those in the controls ( $0.60 \pm 0.16$ ,  $0.46 \pm 0.18$  and  $0.58 \pm 0.21$ , respectively,  $p < 0.05$ ). However, no difference was found in the expression level of MMP-2 gene between the plaques and controls ( $0.88 \pm 0.14$  versus  $0.80 \pm 0.11$ ). It was quite interesting that TFPI-2 gene expression was significantly higher in the controls ( $0.94 \pm 0.23$ ) than that in plaques ( $0.32 \pm 0.08$ ,  $p < 0.01$ ).

As for TIMP genes, the only TIMP-1 gene was significantly upregulated in plaques in comparison with that in the controls ( $1.28 \pm 0.23$  versus  $0.81 \pm 0.10$ ,  $p < 0.05$ ) (Table 2). Among the combination of the ratios of the four MMPs to the three TIMPs examined in this study, the expression ratios of MMP-1 to TIMP-1, MMP-3 to TIMP-3 and MMP-9 to TIMP-1 were significantly higher in plaques than in the controls ( $2.98 \pm 0.77$  versus  $0.99 \pm 0.43$ ,  $2.18 \pm 0.53$  versus  $0.63 \pm 0.22$  and  $1.80 \pm 0.14$  versus  $0.83 \pm 0.09$ , respectively,  $p < 0.05$ ) (Fig. 1). Of interest, in plaques with disruption of fibrous cap, MMP-9 expression ( $3.36 \pm 1.52$ ) and the ratio of MMP-9 to TIMP-1 ( $1.66 \pm 0.12$ ) were significantly higher than those in plaques without disruption ( $1.11 \pm 0.52$  and  $0.76 \pm 0.12$ , respectively), although TFPI-2 gene expression was not different between these groups ( $0.27 \pm 0.08$  versus  $0.40 \pm 0.18$ ).

MMP-9 protein was expressed both in disrupted and non-disrupted plaques, but was not expressed or only slightly expressed in controls. Under these conditions, net expression of MMP-9 was significantly higher in disrupted ( $2.61 \pm 0.17$ ,

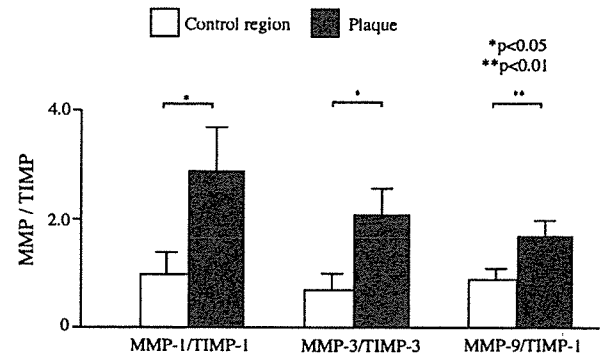


Fig. 1. Imbalanced expression of matrix metalloproteinase (MMP) to tissue inhibitor of matrix metalloproteinase (TIMP) genes in carotid plaque. Vertical axis represented the ratio of MMP/TIMP. Open columns represent values from control regions and closed columns values from plaques.

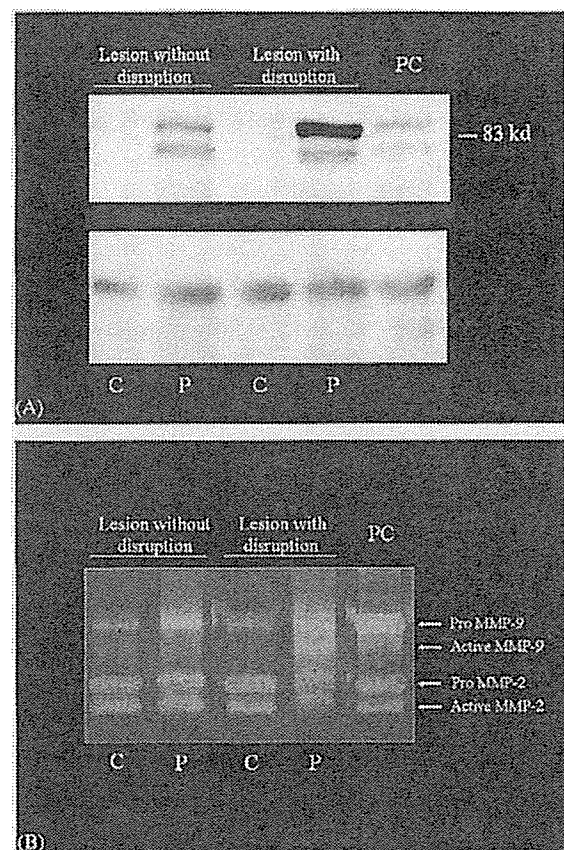


Fig. 2. Expression and function of MMP-9 in protein level. (A) Western blotting for matrix metalloproteinase MMP-9 (upper) and an internal marker protein, endothelin receptor (ETR) (lower), in non-ruptured lesion, ruptured carotid lesions and positive control (PC). MMP-9 was clearly expressed in the plaque (P) and PC, whereas in the control region (C), little expression of MMP-9 was observed. Note that both pro\* and active\*\* form of MMP-9 appears to be highly expressed in the ruptured plaque, in comparison with the non-ruptured plaque, although ETR protein is equally expressed. (B) By zymography, increased size and staining of both pro- and active forms of MMP-9 particularly in ruptured plaques, although MMP-2 activity was not different in each lane as observed in mRNA analysis.

$n=4$ ) than in non-disrupted plaques ( $1.11 \pm 0.12$ ,  $n=6$ ,  $p<0.05$ ), despite the equal expression of an internal marker protein, endothelin-1 receptor (Fig. 2A). Interestingly, the amount of active form MMP-9 determined by zymography was significantly higher in the disrupted ( $2.62 \pm 0.12$ ) than in non-disrupted plaques ( $0.72 \pm 0.07$ ,  $p<0.05$ ), although pro MMP-9 activity was not significantly different in disrupted ( $1.8 \pm 0.10$ ) and non-disrupted plaques ( $1.4 \pm 0.11$ ) (Fig. 2B). There were no significant differences between the levels of pro and active forms of MMP-2, as demonstrated in its mRNA expression.

### 3.3. Immunohistochemistry

In the adjacent control regions (Fig. 3A), there was mild atherosclerosis where a few CD-68 positive macrophages existed. Under these conditions, MMPs and TIMPs were scattering positive. In contrast, TFPI-2 was diffusely positive in the intima and media. Plaque regions mainly consisted of lipid-rich core and fibrous tissue (Fig. 3B) where CD-68 positive macrophages were accumulated particularly in the shoulder regions of atheroma and all MMPs and TIMPs were

strongly positive. It was interesting that, under these conditions, TFPI-2 was regionally positive in the plaque regions. Because of small number of examined plaques, we could not correlate expression of MMPs, TIMPs and TFPI-2 to the stage of plaque development.

## 4. Discussion

### 4.1. Gene expression of MMPs, TIMPs and TFPI-2 in plaque

One of the striking findings of the present study was that with a decreased TFPI-2 gene expression, the MMP-9 gene together with the MMP-9 protein was significantly upregulated in plaques, particularly in plaques with disrupted fibrous cap. Increased production of MMP-9 is thought to contribute to the progressive deterioration of the elastic lamellae associated with vessel remodeling, which could be closely related to the occurrence of plaque disruption [15]. Indeed, previous studies indicated that MMP-9 was present in the coronary plaque from unstable angina [16] and carotid plaque from

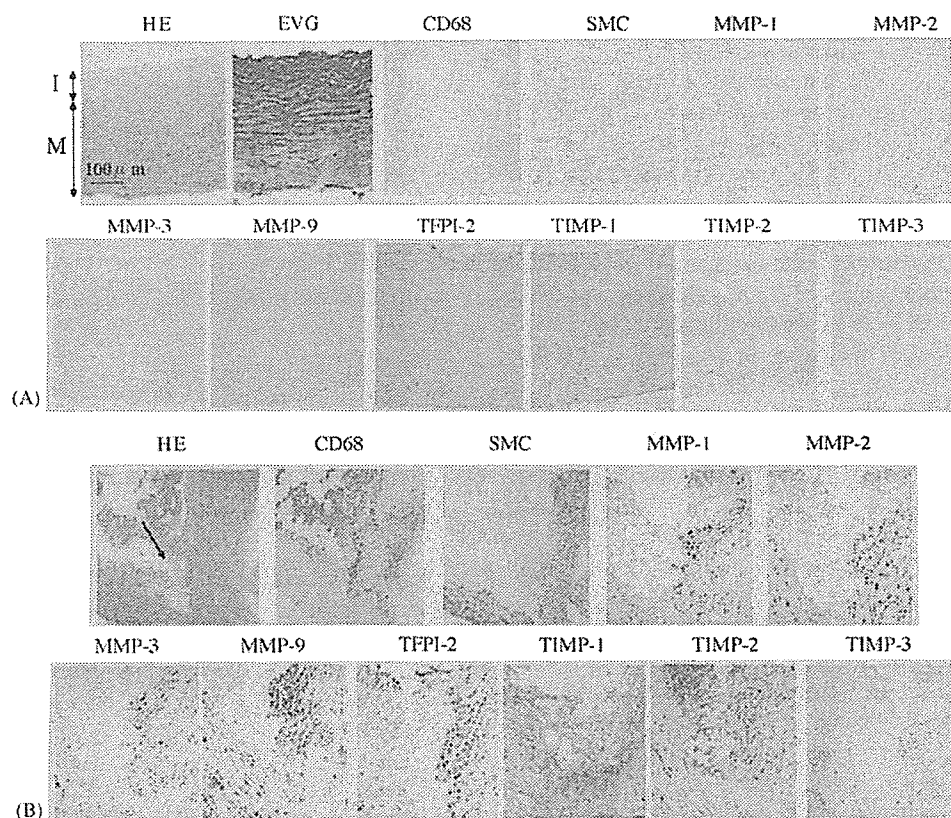


Fig. 3. Histologic and immunohistologic findings (with original magnification of  $\times 25$ ). (A) In the control tissues, there existed mild atherosclerotic lesion where a few CD-68 positive macrophages was found. Under these conditions, tissue factor pathway inhibitor (TFPI)-2 was diffusely positive in the intima and media, although matrix metalloproteinases (MMPs) and tissue inhibitor of MMPs (TIMPs) were scattering positive. An arrow indicates boundary between intima and media. (B) In plaque lesions with a lipid-rich core where CD-68 positive macrophages were accumulated, all MMPs and TIMPs were strongly positive particularly in the shoulder regions of atheroma (arrow). It was interesting that, under these conditions, TFPI-2 was regionally positive in this lesion. EVG, elastica van Gieson; HE, hematoxylin–eosin; I, intima; M, media; SMC, smooth muscle cell.



symptomatic patients [17]. We in fact demonstrated greater upregulation and function of MMP-9 in plaques with fissured fibrous cap at the mRNA as well as protein level, based on histological findings.

Simultaneous upregulation of the MMP-1 and -3 genes was also observed, as previously reported [18,19]. MMP-1 specifically cleaves collagen types I and III, which are key components of the extracellular framework of the arterial wall and major constituents of human atherosclerotic plaques, and activate other MMPs [6] that degrade denatured collagen, gelatin and elastin. MMP-3 has the widest substrate repertoire of all MMPs, showing activity against most of the extracellular proteins and proteoglycans [20]. However, unlike MMP-9, there were no differences in the expression of MMP-1 and -3 genes between plaques with and without rupture. This suggests that simultaneous upregulation of these MMPs is a plausible phenomenon in the development of atherosclerotic plaques.

This study demonstrates diminished gene expression of TFPI-2 in plaques that contain abundant MMPs. TFPI-2, originally considered as a serine proteinase inhibitor, is known to be highly expressed in smooth muscle cells of the relatively non-diseased tissue favoring ECM stability by inactivating collagenases such as MMP-1 as well as gelatinases probably through direct protein/protein interactions. Indeed, Herman et al. [7] demonstrate inverse relation between TFPI and MMP activity in atherosclerotic tissue. Thus, decreased TFPI-2 gene expression in plaques, as observed in the present study, might allow increased matrix degradation by MMP-1, -3 and -9 in plaques, enhancing their susceptibility to plaque development. It is interesting, under these conditions, TIMP-1 exhibited significantly higher expression in plaques than in controls. The combined deletion of TIMP-1 and ApoE in mice leads to a reduction in atherosclerotic plaque size [21], whereas overexpression of TIMP-1 induced by adenovirus-mediated transfer in ApoE-deficient mice leads to a decrease in plaque size and an increase in collagen content [22]. Taken together, under the condition where TFPI-2 was diminished to express, upregulation of TIMP-1 seems to counteract overexpression of MMPs, to exert an inhibitory effect on the development of atherosclerotic plaque.

However, the expression ratios of MMPs to TIMP-1 were still higher in the plaque compared with the control regions. Compensatory expression of TIMP-1 might not be sufficient to counteract the degenerative role of MMPs in the plaque, thus contributing to the development of atherosclerotic plaque. Particularly, the MMP-9/TIMP-1 ratio was significantly higher in plaques with disruption than in those without disruption. This suggests the functional significance of the imbalance of expression of these genes in the occurrence of plaque disruption. It would be of interest to examine which can play a more important role, TFPI-2 or TIMP-1, for the regulation of MMP activity, since compartmentalization might result in distinct microenvironments with corresponding variations in MMP/inhibitor ratios.

#### 4.2. Clinical implications and limitations

A recent experimental study in which local MMP-9 was upregulated by gene transfection resulted in enhanced formation of local thrombus [23]. On the contrary, manipulation to augment expression of expression of TIMPs prevented the occurrence of plaque disruption [22]. Therefore, one might speculate that the altered balance of MMP-9/TIMP-1 with decreased TFPI-2 observed in the present study contributes to plaque disruption associated with or without regional thrombosis.

The carotid plaques examined in the present study were obtained from highly stenotic lesion probably representing the final stage of plaque development and destabilization. In acute coronary syndrome, however, atherosclerotic plaque disruption is known to occur at the sites of mild to moderate stenotic lesions [24] that were not examined in the present study. Although preliminary results indicate that in coronary plaques related to acute coronary syndrome MMP-9 gene was highly expressed in comparison with that in plaques from stable coronary disease [25], further study will need to confirm gene expression in carotid plaque from mild to moderate stenotic lesion.

The present study has a limitation regarding histological assessment of the presence of plaque disruption. Only a small portion of each plaque was examined histologically, and it may well be that features were missed in some patients. Several reports suggest that vulnerability to plaque rupture is a multifocal phenomenon particularly at the time of acute presentation [26,27]. Conversely, one might argue that we did not necessarily determine mRNA expression levels in the part of the plaque where histological analysis was performed. Even under these conditions, imbalanced expression of MMPs/TIMPs with reduction of TFPI-2 was observed in plaques, particularly in those associated with disruption. That the control regions were obtained from adjacent to the culprit lesion is another limitation. However, there was no histological evidence for plaque disruption in the control regions used for present study even in the presence of mild atherosclerosis. It can not be excluded, however, that the disruption of the fibrous cap could be resulted from surgical procedure, although we carefully examined the part of plaque where surgical procedures was not affected.

Whether upregulation of MMPs is the cause or result of plaque disarrangement is unclear. A recent study suggested that MMP-9 might have a protective effect against plaque development in double ApoE and MMP-9 knockout mice [28]. Thus, a causal relationship cannot be concluded until a controlled trial with a specific MMP-9 inhibitor is performed. Recently, MMP-8, traditionally associated only with neutrophils, which enhanced matrix breakdown by activating MMPs and/or by inactivating TIMP-1, was found to be highly expressed in macrophages in disrupted plaques [29]. Reduced expression of TFPI-2 might be related to the enhanced expression of neutrophil elastase in plaques, although MMP-

8 gene expression was not determined in the present study.

In the present study, we used real-time RT-PCR, which gives an estimate of mRNA expression instead of protein level for each enzyme and inhibitor, because it is still difficult to extract some proteases such as MMP-1, which binds strongly to connective tissue and to quantitatively assay enzyme activities [30]. However, it is important to determine the activity of TIMPs in protein level, since determination of gene expression can sometimes misinterpret the actual change of protein expression [31]. Therefore, evaluation of mRNA expression of multiple genes by the present real-time RT-PCR method in combination with determination of protein should be done for systematic evaluation of the activities of MMPs, TIMPs and TFPI-2 in clinical tissue samples.

Finally, the precise mechanism of the sustained overexpression of MMPs and TIMPs with reduction of TFPI-2 in advanced atherosclerotic plaque is still unclear. Our preliminary report indicate that CXCR-2, a chemokine receptor, gene was highly upregulated in accordance with MMP expression in macrophages [32]. This suggests that overexpression of MMPs could be related to a continuous inflammatory reaction, although there was no difference in serum levels of hs-CRP between patients with ruptured and non-ruptured plaques. Further study of the regulatory mechanisms of chemokine and cytokine systems with transcription factors that also play a crucial role in MMP expression [33] may demonstrate a significant pathway for the expression and activation of proteinases and their inhibitors in human atherosclerotic lesions.

## 5. Conclusion

We applied a real-time RT-PCR method to quantitate mRNA expression in small samples of human carotid plaque. Levels of MMP-1, -3, -9 and TIMP-1 mRNAs were significantly upregulated in human carotid plaque where TFPI-2 mRNA was decreased to be expressed. The particular upregulation of MMP-9 and resultant imbalance of MMP-9/TIMP-1 expression could play a pivotal role in plaque disruption.

## Acknowledgements

This work was supported in part by grants from the Ministry of Health, Welfare and Labor of Japan and from the Cardiovascular Research Foundation (to M.Y.), the Promotion of Fundamental Studies in Health Science of the Organization for Pharmaceutical Safety and Research (OPSR) of Japan (to A.S.), and the Japan Cardiovascular Research Foundation (to A.S.). A part of this work was presented at the 53rd Annual Scientific Session, American College of Cardiology, in New Orleans, 2004.

## References

- [1] Falk E, Shah PK, Fuster V. Coronary plaque disruption. *Circulation* 1995;92:657–71.
- [2] Carr S, Farb A, Pearce WH, et al. Atherosclerotic plaque rupture in symptomatic carotid artery stenosis. *J Vasc Surg* 1996;23:755–65.
- [3] Libby P. Inflammation in atherosclerosis. *Nature* 2002;420:868–74.
- [4] Dollery CM, McEwan JR, Henney AM. Matrix metalloproteinases and cardiovascular disease. *Circ Res* 1995;77:863–8.
- [5] Galis ZS, Khatri JJ. Matrix metalloproteinases in vascular remodeling and atherogenesis: the good, the bad, and the ugly. *Circ Res* 2002;90:251–62.
- [6] Nagase H. Activation mechanisms of matrix metalloproteinases. *Biol Chem* 1997;378:151–60.
- [7] Herman MP, Sukhova GK, Kiesel W, et al. Tissue factor pathway inhibitor-2 is a novel inhibitor of matrix metalloproteinases with implications for atherosclerosis. *J Clin Invest* 2001;107:1117–26.
- [8] Fabunmi RP, Sukhova GK, Sugiyama S, et al. Expression of tissue inhibitor of metalloproteinases-3 in human atheroma and regulation in lesion-associated cells: a potential protective mechanism in plaque stability. *Circ Res* 1998;83:270–8.
- [9] Galis ZS, Sukhova GK, Lark MW, et al. Increased expression of matrix metalloproteinases and matrix degrading activity in vulnerable regions of human atherosclerotic plaques. *J Clin Invest* 1994;94:2493–503.
- [10] Brew K, Dinakarpandian D, Nagase H. Tissue inhibitors of metalloproteinases: evolution, structure and function. *Biochim Biophys Acta* 2000;1477:267–83.
- [11] Knox JB, Sukhova GK, Whittemore AD, et al. Evidence for altered balance between matrix metalloproteinases and their inhibitors in human aortic diseases. *Circulation* 1997;95:205–12.
- [12] Sternlicht MD, Werb Z. How matrix metalloproteinases regulate cell behavior. *Annu Rev Cell Dev Biol* 2001;17:463–516.
- [13] Higashikata T, Yamagishi M, Sasaki H, et al. Application of real-time RT-PCR to quantifying gene expression of matrix metalloproteinases and tissue inhibitors of metalloproteinases in human abdominal aortic aneurysm. *Atherosclerosis* 2004;177:353–60.
- [14] Kolodgie FD, Burke AP, Farb A, et al. The thin-cap fibroatheroma: a type of vulnerable plaque, the major precursor lesion to acute coronary syndrome. *Curr Opin Cardiol* 2001;16:285–92.
- [15] Schoenhagen P, Ziada KM, Kapadia SR, et al. Extent and direction of arterial remodeling in stable versus unstable coronary syndromes: an intravascular ultrasound study. *Circulation* 2000;101:598–603.
- [16] Brwon DL, Hibbs MS, Kearney M, et al. Identification of 92-kD gelatinase in human coronary atherosclerotic lesions. Association of active enzyme synthesis with unstable angina. *Circulation* 1995;91:2125–31.
- [17] Loftus IM, Naylor AR, Goodall S, et al. Increased matrix metalloproteinase-9 activity in unstable carotid plaques. A potential role in acute plaque disruption. *Stroke* 2000;31:40–7.
- [18] Nikkari ST, O'Brien KD, Ferguson M, et al. Intestinal collagenase (MMP-1) expression in human carotid atherosclerosis. *Circulation* 1995;92:1393–8.
- [19] Sukhova GK, Schonbeck U, Rabkin E, et al. Evidence for increased collagenolysis by interstitial collagenases-1 and -3 in vulnerable atheromatous plaques. *Circulation* 1999;99:2503–9.
- [20] Sato H, Takino T, Okada Y, et al. A matrix metalloproteinase expressed on the surface of invasive tumor cells. *Nature* 1994;370:61–5.
- [21] Silence J, Collen D, Lijnen HR. Reduced atherosclerotic plaque but enhanced aneurysm formation in mice with inactivation of the tissue inhibitor of metalloproteinase-1 (TIMP-1) gene. *Circ Res* 2002;90:897–903.
- [22] Rouis M, Adamy C, Duverger N, et al. Adenovirus-mediated overexpression of tissue inhibitor of metalloproteinase-1 reduces atherosclerotic lesions in apolipoprotein E-deficient mice. *Circulation* 1999;100:533–40.

- [23] Morishige K, Shimokawa H, Matsumoto Y, et al. Overexpression of matrix metalloproteinase-9 promotes intravascular thrombus formation in porcine coronary arteries in vivo. *Cardiovasc Res* 2003;57:572–85.
- [24] Yamagishi M, Terashima M, Awano K, et al. Morphology of vulnerable coronary plaque: insights from follow-up of patients examined by intravascular ultrasound before an acute coronary syndrome. *J Am Coll Cardiol* 2000;35:106–11.
- [25] Higo S, Nanto S, Higashikata T, et al. Impact of altered expression balance of matrix metalloproteinases and tissue inhibitor of metalloproteinases genes on coronary plaque rupture: results from quantitative tissue analysis using real-time reverse transcriptase-polymerase chain reaction method (abstr). *J Am Coll Cardiol* 2004;43(Suppl. A):257A.
- [26] Rioufol G, Finet G, Ginon I, et al. Multiple atherosclerotic plaque rupture in acute coronary syndrome. A three-vessel intravascular ultrasound study. *Circulation* 2002;106:804–8.
- [27] Schoenhagen P, Stone GW, Nissen SE, et al. Coronary plaque morphology and frequency of ulceration distant from culprit lesions in patients with unstable and stable presentation. *Arterioscler Thromb Vasc Biol* 2003;23:1895–900.
- [28] Johnson J, George A, Newby C. Matrix metalloproteinase-9 and -12 have opposite effects on atherosclerotic plaque stability (abstr). *Atherosclerosis* 2003;4(Suppl.):196.
- [29] Dollery CM, Owen CA, Sukhova GK, et al. Neutrophil elastase in human atherosclerotic plaques. Production by macrophages. *Circulation* 2003;107:2829–36.
- [30] Woessner JR. Quantification of matrix metalloproteinases in tissue samples. *Methods Enzymol* 1995;248:510–28.
- [31] Blindt R, Vogt F, Lamby D, et al. Characterization of differential gene expression in quiescent and invasive human arterial smooth muscle cells. *J Vasc Res* 2002;39:340–52.
- [32] Yamagishi M, Higashikata T, Higashi T, et al. Sustained upregulation of chemokine and its receptor genes associated with matrix metalloproteinase overexpression in human carotid plaque rupture: results from a quantitative study with real-time reverse transcriptase-polymerase chain reaction method (abstr). *J Am Coll Cardiol* 2004;43(Suppl.):497A.
- [33] Chase AJ, Bond M, Crook MF, et al. Role of nuclear NF- $\kappa$ B activation in metalloproteinase-1 -3 and -9 secretion by human macrophages in vitro and rabbit form cells produced in vivo. *Arterioscler Thromb Vasc Biol* 2002;22:765–71.

## Outcome of carotid endarterectomy and stent insertion based on grading of carotid endarterectomy risk: a 7-year prospective study

KOJI IIHARA, M.D., PH.D., KENICHI MURAO, M.D., PH.D., NOBUYUKI SAKAI, M.D., PH.D., NAOAKI YAMADA, M.D., PH.D., IZUMI NAGATA, M.D., PH.D., AND SUSUMU MIYAMOTO, M.D., PH.D.

*Departments of Neurosurgery and Radiology, National Cardiovascular Center, Osaka, Japan*

**Object.** The authors of this study prospectively compared periprocedural neurological morbidity and the appearance of lesions on diffusion-weighted (DW) magnetic resonance (MR) imaging in patients who had undergone carotid endarterectomy (CEA) or carotid artery stent placement (CASP) with distal balloon protection, based on a CEA risk grading scale.

**Methods.** Patients undergoing CEA (139 patients) and CASP (92 patients) were classified into Grades I to IV, based on the presence of angiographic (Grade II), medical (Grade III), and neurological (Grade IV) risks. Although not randomized, the CEA and CASP groups were well matched in terms of the graded risk factors except for a greater proportion of neurologically unstable patients in the CEA group (11 compared with 3%,  $p = 0.037$ ). There were greater proportions of asymptomatic (64 compared with 34%,  $p = 0.006$ ) and North American Symptomatic Carotid Endarterectomy Trial–ineligible patients (29 compared with 14%,  $p < 0.0001$ ) in the CASP group. The overall rates of neurological morbidity with ischemic origin and the appearance of lesions on DW MR imaging after CEA were 2.2 and 9.3%, and those after CASP were 7.6 and 35.9% (nondisabling stroke only), respectively. The only disabling stroke was caused by an intracerebral hemorrhage attributable to hyperperfusion in one case (0.7%) of CEA. There were no deaths. There was no significant association between neurological morbidity and the risk grade in patients who had undergone CEA, although the incidence of lesions on DW imaging was significantly greater in the Grade IV risk group compared with that in the other risk groups combined (42.1 compared with 4.2%,  $p < 0.0001$ ). After CASP, a higher incidence of neurological morbidity and lesions on DW imaging was noted for the Grade II and III risk groups combined as compared with that in the Grade I risk group, regardless of a symptomatic or an asymptomatic presentation (neurological morbidity: 10.5 compared with 3.1%, respectively,  $p = 0.41$ ; and DW imaging lesions: 47.4 compared with 19.4%,  $p = 0.01$ ). The incidence of lesions on DW imaging after CEA was significantly lower than that after CASP except for the Grade IV risk groups.

**Conclusions.** Despite a higher incidence of DW imaging–demonstrated lesions in the Grade IV risk group, there was no significant association between the risk group and neurological morbidity rates after CEA. The presence of vascular and medical risk profiles conferred higher rates of neurological morbidity and an increased incidence of lesions on DW imaging after CASP. Considering that no serious nonneurological complications were noted, CEA and CASP appear to be complementary methods of revascularization for carotid artery stenosis with various risk profiles.

**KEY WORDS** • carotid stenosis • diffusion-weighted imaging • endarterectomy • angioplasty • stent • risk factor

CAROTID endarterectomy is the gold standard treatment for both symptomatic and asymptomatic CA stenosis.<sup>1–4</sup> The efficacy of this procedure in the prevention of stroke has been established in several randomized clinical trials,<sup>1–4</sup> and its long-term effectiveness has also been reported.<sup>13</sup> It is important to note, however, that this

efficacy has been proven only in a subgroup of patients selected according to various criteria.<sup>1–4</sup> In recent years, stent implantation has been developed as an alternative to CEA for high-grade stenosis in the CAs.<sup>37</sup> Although its long-term efficacy in preventing stroke has not been established, CASP is, in principle, indicated in high-risk patients.<sup>23,26,32</sup> Nevertheless, the quest for less invasive therapeutic alternatives has led to a gradual increase in the number of CASPs performed not only in high-risk patients but also in others.<sup>36</sup> Several large randomized studies are now in progress to compare the safety and efficacy of CEA and CASP for the prevention of stroke in specifically defined patients.<sup>10,15,20,38</sup> To date, several factors have been

*Abbreviations used in this paper:* CA = carotid artery; CASP = CA stent placement; CCA = common CA; CEA = carotid endarterectomy; DW = diffusion-weighted; ICH = intracerebral hemorrhage; MR = magnetic resonance; NASCET = North American Symptomatic Carotid Endarterectomy Trial; TIA = transient ischemic attack.



## Outcome based on carotid endarterectomy risk

shown to correlate with poor outcome after CASP.<sup>7,24,28</sup> It is important to note that classifying CA stenosis cases as high-risk for surgical intervention has been traditionally based on risks previously revealed in large CEA studies. In no previous study, however, have authors systematically compared periprocedural morbidity and cerebral embolization rates after CEA and CASP based on the CEA risk grading scale established by Sundt and colleagues.<sup>33</sup> In the present study we prospectively compared the neurological risks of CEA and CASP, according to this scale.

### Clinical Material and Methods

#### *Patient and Disease Characteristics*

Between September 1998 and August 2004, 205 patients (187 men) with a mean age of  $69.4 \pm 6.7$  years underwent 231 procedures for CA stenosis (139 CEAs and 92 CASPs); lesions caused symptoms in 54.1% of cases. The patients were prospectively registered, and Grades I to IV based on the CEA Risk Grading Scale were assigned.<sup>33</sup> Carotid endarterectomy was considered the first line of therapy; CASP was indicated mainly in high-risk patients (including those who were ineligible for NASCET), in those with echogenic plaque, and in those who expressed a preference for the procedure. Considering its extremely high surgical risk, recurrent stenosis post-CEA was a definite indication for CASP in this study. An advanced age was defined as 75 years or older.<sup>25</sup> The degree of CA stenosis was measured on digital subtraction angiography according to the method used in the NASCET,<sup>17</sup> and the indications for intervention were as follows: for symptomatic cases, 70% or greater stenosis; and for asymptomatic cases, 75% or greater stenosis. The nature of CA plaque was assessed using duplex ultrasonography. Echolucent plaques are predominantly composed of atheromatous debris, lipids, and intraplaque hemorrhage, whereas echogenic plaques mainly consist of more stable fibrous tissue.<sup>18</sup> Plaques with echolucent areas are more unstable and prone to fragmentation and embolization than are echogenic plaques.

#### *Neurological Complications*

The incidence of neurological complications 30 days postprocedure was calculated based on the CEA risk grade in patients assigned to either treatment group. Neurological deficits other than TIA were classified as nondisabling (that is, a new neurological deficit persisting for more than 24 hours but a modified Rankin Scale score  $< 3$  at 30 days posttreatment) or disabling stroke (modified Rankin Scale score  $\geq 3$  at 30 days posttreatment).

#### *Imaging Studies*

Preoperative digital subtraction angiography was routinely performed except in one case involving an 83-year-old patient who underwent a CEA before the repair of an abdominal aortic aneurysm. The incidence of new periprocedural ischemic events, based on the CEA risk grade, was determined by comparing preoperative images with DW MR images (MAGNETOM Vision; Siemens AG, Munich, Germany) that had been obtained between 2 and 4 days after treatment. All imaging studies were performed according to the following protocol: TE 100 msec, field of view  $23 \times 23$  cm, matrix  $98 \times 128$ , slice thickness 4 mm, and

b value 1000 seconds/mm<sup>2</sup>. When staged interventions were planned in cases of CA and coronary artery lesions, DW MR imaging studies were performed just before and after carotid revascularization to accurately assess cerebral ischemic events caused by carotid interventions.

#### *Therapeutic Procedure*

Carotid endarterectomy was performed while the patient was in a state of general anesthesia by using an operating microscope and somatosensory evoked potential monitoring to selectively place the shunt. In cases of CASP, patients had been given antiplatelet agents (aspirin 81–100 mg daily, ticlopidine 200 mg daily, cilostazol 200 mg daily, either alone or in combination) at least 48 hours before the insertion procedure, which was performed after the application of a local anesthetic agent. An intravenous heparin bolus (5000 U) was given to elevate the activated clotting time between 2- and 2.5-fold above baseline values. A No. 6-9 French guiding catheter was advanced into the CCA and placed proximal to the stenosis. A flexible guidewire (diameter 0.14 inch) or GuardWire Plus (Medtronic AVE, Minneapolis, MN) was advanced through the guiding catheter and navigated across the stenosis. The vessel was predilated with a percutaneous transluminal angioplasty balloon catheter placed across the stenosis. A balloon-expandable or self-expandable stent was then placed across the dilated segment over the guidewire by using a stent delivery system. The stents used were Palmaz (Johnson and Johnson, New Brunswick, NJ), EasyWall (Boston Scientific, Osaka, Japan), SMART or SMARTeR (Cordis, Miami Lakes, FL), Acculink (Guidant, Tokyo, Japan), Xpert (Abbott Vascular Devices, Tokyo, Japan), and others in two, 12, 72, 11, one, and two cases, respectively.

Before April 2003 (CASP I), the cerebrum was protected from distal embolism during the postdilation stage of the placement procedure by using a silicone balloon (Kaneka Medix, Kanagawa, Japan).<sup>34</sup> In the 18 cases treated since May 2003 (CASP II), CASP was usually performed under total protection, if possible, by using a GuardWire Plus system, temporary occlusion, and an aspiration system. Three surgeons and two interventionists in a single neurosurgical team performed the CEA and CASP procedures, respectively, during the study period.

#### *Statistical Analysis*

Differences between groups were evaluated using the chi-square or Fisher exact test (for categorical variables) and t-tests (for continuous variables). Two-sided probability values less than 0.05 were considered significant. Statistical analysis was performed using a commercially available computer software package (JMP, version 5.1.1; SAS Institute, Cary, NC).

### Results

The CEA and CASP groups were similar with regard to sex and medical history despite the following differences (Table 1): the mean age of patients who had undergone CASP was significantly greater than that of those who had undergone CEA, and approximately double the number of patients who underwent CASP had had an asymptomatic presentation compared with those who underwent CEA.

TABLE 1

Demographics of patients assigned to each treatment group\*

Parameter	Value (%)		p Value
	CEA	CASP	
no. of patients	139	92	
age (yrs)			
mean $\pm$ SD	68.1 $\pm$ 6.9	71.3 $\pm$ 6.0	<0.001
range	43–82	55–83	
male sex	128 (92.0)	83 (90.2)	0.621
medical history			
DM	47 (33.8)	37 (40.2)	0.322
hyperlipidemia	15 (10.8)	16 (17.5)	0.150
hypertension	103 (74.1)	68 (73.9)	0.975
CAD	46 (33.1)	35 (38.0)	0.440
current smoker or history of smoking	71 (51.1)	40 (43.5)	0.257
PVD	65 (46.8)	41 (44.6)	0.743
target carotid stenosis, asymptomatic presentation	47 (33.8)	59 (64.1)	<0.0001
NASCET-ineligible cases			
overall	20 (14.4)	27 (29.3)	0.006
symptomatic	15 (16.3)	8 (24.2)	0.313
asymptomatic	5 (10.6)	19 (32.2)	0.008
CEA risk grade†			
I	63 (45.3)	32 (34.8)	
II	15 (10.8)	10 (10.9)	
III	42 (30.2)	47 (51.1)	
IV	19 (13.7)	3 (3.3)	

\* CAD = coronary artery disease (angina pectoris or a recent myocardial infarction within 6 months); DM = diabetes mellitus; PVD = peripheral vascular disease; SD = standard deviation.

† CEA risk grades: I, neurologically stable patients with no major medical or angiographically defined risks but with unilateral or bilateral ulcerative/stenotic CA disease; II, neurologically stable patients with no major medical risks but with significant angiographically defined risks; III, neurologically stable patients with major medical risks and with or without significant angiographically defined risks; and IV, neurologically unstable patients with or without associated major medical or angiographically defined risks.

TABLE 2

Main reasons for selecting CASP, according to the CEA risk grades\*

CEA Risk Grade	Total No. of Patients	Reasons for CASP	No. of Patients
I	32	NASCET exclusion criteria	13
		restenosis post-CEA	7
		nonatheromatous stenosis	2
		cardiac valvular or rhythm disorder	2
		surgical inaccessibility	1
		previous disabling stroke	1
		asymptomatic, patient preference	12
		symptomatic, echogenic plaque	6
		symptomatic, patient preference	1
		asymptomatic, patient preference	6
II	9	NASCET exclusion criteria	2
		restenosis post-CEA	1
		tandem stenosis	1
		symptomatic, patient preference	1
		advanced age (>75 yrs)	22
		NASCET exclusion criteria	9
		restenosis post-CEA	2
		age >79 yrs	1
		cardiac valvular or rhythm disorder	1
		urgent CABG	1
III	47	recent MI	1
		surgical inaccessibility	1
		renal failure	1
		nonatheromatous stenosis	1
		angina pectoris	9
		severe PVD	6
		congestive heart failure	1
		NASCET exclusion criteria	2
		recent MI	1
		age >79 yrs	1
IV	3	advanced age (>75 yrs)	1

\* The most important reason for the therapeutic choice is listed for each patient. Abbreviations: CABG = coronary artery bypass graft; MI = myocardial infarction.

Furthermore, a larger proportion of patients who had undergone CASP were NASCET-ineligible. The distribution of patients based on the grading scale by Sundt and colleagues significantly differed between the two treatment groups ( $p = 0.005$ ): those with a Grade III risk composed approximately one half of the patients who had undergone CASP, whereas those with a Grade I risk composed approximately one half of those who had undergone CEA. Table 2 shows the main reasons for selecting CASP for each risk grade. In the Grade I risk group, CASP was indicated mainly in NASCET-ineligible cases or in patients with asymptomatic lesions who had expressed a preference for the procedure. An advanced age and NASCET exclusion criteria were the main reasons for selecting CASP in the higher risk grades.

Table 3 shows the details of the risk factors as defined according to the grading system by Sundt and colleagues. The incidence of risk profiles was similar between the two procedures, except for the greater proportion of patients who had presented with frequent TIA in the CEA group.

The overall rate of periprocedural neurological morbidity after CEA was 2.9% (disabling stroke 0.7% and nondisabling stroke 2.2%), with rates of 3.3 and 2.1% for symptomatic and asymptomatic cases, respectively. The overall

rate of periprocedural neurological morbidity after CASP was 7.6% (nondisabling stroke only), with rates of 6.1 and 8.5% for symptomatic and asymptomatic cases, respectively. The incidence of ICH due to hyperperfusion syndrome was 0.4% (one case). The only disabling stroke resulted from an ICH into the previous ipsilateral cortical infarct and was caused by hyperperfusion on Day 4 after CEA for symptomatic stenosis with contralateral CA occlusion in a patient with a Grade II risk. A visual deficit caused by retinal embolism developed in two patients (2.2%) who had undergone CASP. The incidence of new DW MR imaging–demonstrated lesions in the CEA and CASP groups was 9.4 and 34.8%, respectively. All cases of periprocedural neurological morbidity, except the case of ICH, were associated with new lesions visualized on DW MR imaging, suggesting that these lesions had an ischemic origin. In both the CEA and CASP groups, symptomatic deficits were noted in approximately one fourth of the cases with new DW imaging abnormalities. Because there was a selection bias in assigning patients to the CEA and CASP groups based on the CEA risk grades, statistical analysis of the overall results was

## Outcome based on carotid endarterectomy risk

not performed. There were no cases of acute myocardial infarction and no deaths.

### Neurological Morbidity of Ischemic Origin and Cerebral Embolization Rates

The overall rate of ischemic neurological morbidity after CEA was 2.2% (nondisabling stroke only). Neurological morbidity of ischemic origin after CEA was noted in two cases with a Grade III risk and one case with a Grade IV risk. There was no significant association between the risk grade and neurological morbidity rates among patients who had undergone CEA ( $p = 0.268$ ). Regarding DW imaging abnormalities (Table 4), there was no significant difference in the number of new lesions detected after CEA among Grades I to III risk groups ( $p = 0.419$ ). In contrast, patients with a Grade IV risk who had undergone CEA had a higher incidence of lesions on DW imaging compared with patients in the other risk groups (42.1 compared with 4.2%,  $p < 0.0001$ ).

All of the cerebral complications after CASP (seven cases) consisted of nondisabling ischemic stroke. Five cases were in the Grade III risk group, and one case each was in the Grades I and II risk groups (Table 4). A higher incidence of neurological deficits occurred in the CASP group among patients with angiographic or medical risks (10 and 10.6% for Grades II and III, respectively) compared with those without any risks (3.1% for Grade I;  $p = 0.414$ ). The incidence of cerebral embolic events after CASP as detected on DW images was significantly different among the risk grades ( $p = 0.028$ ); the incidence for risk Grades II and III combined was significantly higher than that for risk Grade I (45.6 compared with 18.8%, respectively,  $p = 0.011$ ). Results of a subgroup analysis comparing CEA and CASP for each risk grade showed a higher incidence of lesions on imaging after CASP for Grades I ( $p = 0.016$ ), II ( $p = 0.017$ ), and III ( $p < 0.001$ ) but not for Grade IV ( $p = 0.273$ ). Despite a higher incidence of neurological morbidity after CASP for risk Grades I to III, this difference was not significant.

The introduction of the GuardWire Plus tended to decrease the overall rates of neurological complications (CASP I, 8.1%; CASP II, 5.6%;  $p = 1.000$ , not significant) as well as the overall rates of cerebral ischemic events on DW MR imaging (CASP I, 37.8%; CASP II, 22.2%;  $p = 0.212$ , not significant), although this difference did not reach statistical significance given the small number of cases. This tendency was noted chiefly in the Grade I risk group, but there seems to be virtually no effect in the Grade III risk group.

### Management Outcome Based on Presentation

Results of the comparisons of periprocedural neurological morbidity and embolic event rates for both symptomatic and asymptomatic cases are listed in Table 5. Regardless of the case presentation, symptomatic or asymptomatic, vascular (Grade II) and medical (Grade III) risk profiles were associated with a higher incidence of neurological morbidity and ischemic lesions on DW MR imaging after CASP, compared with the baseline risk (Grade I). There was a significant difference in the incidence of DW imaging abnormalities between the CEA and CASP groups among Grade III risk groups with either symptomatic ( $p = 0.001$ ) or asymptomatic presentation ( $p = 0.026$ ).

TABLE 3

Summary of CEA risk factors in patients assigned to CEA and CASP\*

Parameter	Value (%)		p Value
	CEA	CASP	
no. of patients			
angiographic risk			
contralateral ICAO	11 (7.9)	12 (13.0)	0.202
siphon stenosis	12 (8.6)	8 (8.7)	0.987
high bifurcation ( $\geq C_2$ )	4 (2.9)	3 (3.3)	1.000†
long lesion‡	5 (3.6)	0	0.160†
intraluminal thrombus	1 (0.7)	0	1.000†
medical risk			
advanced age ( $\geq 75$ yrs)	24 (17.3)	25 (27.2)	0.071
CAD	26 (18.7)	19 (20.7)	0.715
severe PVD	7 (5.0)	9 (9.8)	0.164
severe HTN ( $> 180/110$ mm Hg)	2 (1.4)	0	0.519†
COPD	1 (0.7)	1 (1.1)	1.000†
CHF	0	1 (1.1)	0.398†
neurological risk			
frequent TIA	15 (10.8)	3 (3.3)	0.037§
general cerebral ischemia	5 (3.6)	3 (3.3)	1.000†
recent CVD (w/in 7 days)	2 (1.4)	0	0.519†

\* CHF = chronic heart failure; COPD = chronic obstructive pulmonary disease; CVD = cerebrovascular disease; HTN = hypertension; ICA = internal carotid artery; ICAO = ICA occlusion.

† Fisher exact test.

‡ That is, extension of the plaque greater than 3 cm distally in the ICA or 5 cm proximally in the CCA.

§ Statistically significant.

### Summary of Periprocedural Ischemic Stroke After Carotid Revascularization

Ischemic complications after CEA were caused by distal embolism during shunt insertion for high-positioned, unstable, ulcerated plaque in a symptomatic patient with cardiac comorbidity (Grade III risk) and by migration of a giant floating thrombus during the dissection phase in an asymptomatic woman with contralateral CCA occlusion (Grade III risk). The remaining complication occurred in a neurologically unstable patient who had recently had a stroke showing severe tandem siphon stenosis and moderate contralateral carotid stenosis (Grade IV risk).

Patient characteristics and presumed specific causes of stroke, if present, after CASP are listed in Table 6. The most striking features in these complicated cases, regardless of the risk grade, included the presence of severe atherosclerotic changes such as contralateral CA occlusion, bilateral severe stenosis, tandem stenosis, and cardiac comorbidities. The specific cause of stroke in a diabetic woman with cardiac comorbidity was presumed to be embolism that had occurred during placement of the guiding catheter for recently progressive CCA stenosis. Acute CA stent thrombosis was responsible for complications in two cases classified as lower risk (Grades I and II). Note that recurrent stenosis post-CEA (10 cases including one symptomatic case) was not associated with any neurological morbidity, and there was no incidence of DW imaging abnormalities.

Nonneurological complications are featured in Table 7. There was a significantly higher incidence of transient, but not permanent, cranial nerve palsy in the CEA group and a higher incidence of hypotension and bradycardia in the CASP group.

TABLE 4  
Incidence of complications and DW MR imaging abnormalities after carotid revascularization, according to the CEA risk grade and surgical procedure

CEA Risk Grade	No. of Cases/Subgroup Total (%)					
	CEA	CASP	p Value	CASP I	CASP II	p Value
no. of patients	139	92		74	18	
<i>incidence of ischemic neurological complications*</i>						
I	0/63 (0)	1/32 (3.1)	0.337	1/27 (3.7)	0/5 (0)	1.000
II	0/15 (0)	1/10 (10)	0.400	1/9 (16.7)	0/1 (0)	1.000
III	2/42 (4.8)	5/47 (10.6)	0.439	4/36 (11.1)	1/11 (9.1)	1.000
IV	1/19 (5.3)	0/3 (0)	1.000	0/2 (0)	0/1 (0)	—
<i>incidence of new abnormalities on DW MR imaging</i>						
I	2/63 (3.2)	6/32 (18.8)	0.016	6/27 (22.2)	0/5 (0)	0.555
II	0/15 (0)	4/10 (40.0)	0.017	4/9 (44.4)	0/1 (0)	1.000
III	3/42 (7.1)	22/47 (46.8)	<0.001	18/36 (50.0)	4/11 (36.4)	0.428
IV	8/19 (42.1)	0/3 (0)	0.273	0/2 (0)	0/1 (0)	—

\* All of the ischemic complications were nondisabling stroke. — = not applicable.

### Discussion

This study provided a unique opportunity to compare in detail the results of CEAs and CASPs by using neurological complication rates and the incidence of lesions on DW MR imaging as outcome measures, according to the CEA risk classification. Authors of recent reports have suggested that CASP can be performed with periprocedural complication rates similar to those for CEA.<sup>22,36</sup> Note, however, that most studies on the safety and efficacy of CASP have included both symptomatic and asymptomatic patients and that varying definitions of stroke as clinical end points make direct comparisons of study results difficult. The grading scheme by Sundt and colleagues<sup>33</sup> is the only empirical system that is based on the degree of neurological stability and the presence of a set of medical and angiographic risk factors for grouping patients. It provides a means of preoperatively evaluating the risks involved in CEA,<sup>25,33</sup> and thus facilitates a systematic comparison of outcomes after CEA and CASP in patients with different surgical risks. We were also able to analyze these outcomes in symptomatic and asymptomatic patients separately for each risk grade, and therefore to address one of the major limitations of the system by Sundt and colleagues.

Although not randomized, the CEA and CASP groups were well matched, except for the greater number of symptomatic patients in the CEA group and NASCET-ineligible patients in the CASP group. These differences are explained by the referral patterns and our therapeutic choice of investigational CASP during the study period. Note, however, that there was no significant difference between the two treatment groups with regard to the CEA risks defined by the grading system, except for the greater number of patients with frequent TIA in the CEA group. This fact reflects an uncertainty about the superiority of either treatment based on the CEA risk profiles.

#### Management Outcome Based on CEA Risk

The risk of stroke and death resulting from CEA is related to a number of patient characteristics, particularly the presence and nature of recent cerebrovascular events.<sup>9,33</sup> The overall outcomes after CEA in the present study were

excellent, and there was no significant association between risk grades and neurological morbidity after CEA. This fact may be explained by our thorough preoperative assessment of medical conditions and plaque characteristics, proper use of  $\beta$ -blocking agents in patients with cardiac comorbidity, and meticulous dissection under transcranial Doppler monitoring of the CA with vulnerable plaques, especially in neurologically unstable patients. The fact that the only disabling stroke was caused by an ICH attributable to hyperperfusion underscores the increasing effect of this problem, although rare, on the overall outcomes of carotid revascularization.<sup>5,11</sup>

The overall neurological morbidity rates and lesion incidence on DW imaging after CASP were relatively higher than those after CEA. Results of a subgroup analysis of CASP cases demonstrated higher neurological complication rates in the high-risk subset (Grades II and III). The introduction of a newer total protection system tended to decrease the overall rate of adverse neurological outcomes to 5.6%, especially in the Grade II risk group. Note, however, that neurological complication rates as well as the incidence of lesions on DW imaging after CASP for the Grade III risk group remained relatively high despite the use of advanced distal protection techniques.

#### Cerebral Embolic Events Detected on DW MR Imaging

Diffusion-weighted MR imaging was used to compare the incidence of ischemic lesions, given that it can detect hyperacute ischemic lesions and differentiate recent acute stroke from old ischemic lesions.<sup>35</sup> Results of the present study clearly showed different incidences of DW imaging abnormalities between the CEA and CASP treatment groups, based on the CEA risk grade. Not surprisingly, the incidence of bright lesions on DW MR images after CEA for cases with Grade IV risks was significantly higher than that for the other grades combined, which agrees with the hypothesis that the majority of neurological complications after CEA have an embolic origin.<sup>16</sup> Note, however, that the incidence of DW imaging abnormalities after CASP was relatively high—approximately 20% even in the lowest risk group (Grade I). In Grades II and III risk groups, the incidence of lesions was more than double the baseline inci-